

## Supporting Information

# Suppressing carbon corrosion via mechanically mixing transition metal phosphide clusters: a comparative *in-situ* study in alkaline media

Xiaoyu Wu,<sup>1,2</sup> Kai Zhao,<sup>1,2</sup> Xiaoyu Yan,<sup>1,2</sup> Xiaojuan Cao,<sup>1,2</sup> Le Ke,<sup>1,2</sup> Yang Zhao,<sup>1,2</sup>  
Lingjiao Li,<sup>1,2</sup> Xiaoyi Jiang,<sup>1,2</sup> and Ning Yan<sup>1,2\*</sup>

1. Key Laboratory of Artificial Micro- and Nano-Structures of Ministry of Education, School of Physics and Technology, Wuhan University, Wuhan 430072, China
2. Shenzhen Research Institute of Wuhan University, Shenzhen, 518057, China

### Corresponding Author

\*E-mail: [ning.yan@whu.edu.cn](mailto:ning.yan@whu.edu.cn)

### This file contains:

1. Materials synthesis procedures
2. Materials characterizations
3. Electrochemical measurement procedures
4. Differential electrochemical mass spectrometry (DEMS)
5. Supporting Figures S1-S16

## 1. Materials synthesis procedures

All chemical reagents and materials, including  $\text{Co}(\text{NO}_3)_2 \cdot 6\text{H}_2\text{O}$ ,  $\text{Fe}(\text{NO}_3)_3 \cdot 9\text{H}_2\text{O}$ ,  $\text{NaH}_2\text{PO}_2 \cdot \text{H}_2\text{O}$ ,  $(\text{MgCO}_3)_4\text{Mg}(\text{OH})_2$ ,  $\text{N}(\text{CH}_2\text{COOH})_3$ ,  $\text{CO}(\text{NH}_2)_2$  and  $\text{NH}_4\text{F}$ , were of analytical grade and used without further purification. And these reagents above were purchased from Aladdin. Nafion solution was produced by E.I. Du Pont; Vulcan XC-72R and platinum on carbon (Pt/C) were from Cabot Corp. PTFE was provided by Cobetter, and high purity argon Ar (99.999%) was provided by Wuhan Zhongyixing Chemical Technology Co., LTD. Deionized water (DI) was used in the synthesis.

### 1.1. Preparation of porous nitrogen-doped carbon (NC)

NC was synthesized based on our previous work.<sup>1</sup> Briefly, nitrilotriacetic acid and magnesium carbonate were dissolved in water at 85 °C. The solution was then quenched by ice bath in which ethanol was added to increase the yield of the magnesium nitrilotriacetate (MgNTA) precipitate. MgNTA was then pyrolyzed at 900 °C in argon flow, the obtained carbon was finally washed by acid to remove the enclosed MgO which served as the pore-former.

### 1.2. FeP-CoP + C and FeP-CoP + NC synthesis:

Firstly, 2 mmol  $\text{Fe}(\text{NO}_3)_3 \cdot 9\text{H}_2\text{O}$ , 2 mmol  $\text{Co}(\text{NO}_3)_2 \cdot 6\text{H}_2\text{O}$ , 20 mmol urea and 8 mmol  $\text{NH}_4\text{F}$  were dissolved in 15 mL deionized water to form a pink solution, followed by vigorous stirring for 20 min. Transfer the pink solution to a Teflon-lined stainless steel autoclave (25mL). The autoclave was sealed and kept in the oven at 120 °C for 12 hours. After the autoclave was cooled to room temperature, the suspension in the autoclave was filtrated to obtain  $\text{Fe}(\text{OH})_3\text{-Co}(\text{OH})_2$  precursor. Then it was dried in a vacuum oven at 60 °C for 5 h. Then,  $\text{NaH}_2\text{PO}_2 \cdot \text{H}_2\text{O}$  and  $\text{Fe}(\text{OH})_3\text{-Co}(\text{OH})_2$  precursors were placed in two small porcelain boats in quartz tubes, and  $\text{NaH}_2\text{PO}_2 \cdot \text{H}_2\text{O}$  porcelain boats were placed upstream. A porcelain boat with  $\text{Fe}(\text{OH})_3\text{-Co}(\text{OH})_2$  precursor was placed downstream (mass ratio of  $\text{NaH}_2\text{PO}_2 \cdot \text{H}_2\text{O}$  to  $\text{Fe}(\text{OH})_3\text{-Co}(\text{OH})_2$  was 10:1). Under the protection of argon atmosphere, the quartz tube was heated to 350 °C at 2 °C per minute to enable the thermal decomposition of  $\text{NaH}_2\text{PO}_2$  and to generate  $\text{PH}_3$  gas. The phosphidation was maintained at 350 °C for 3 h. The mechanical mixing of FeP-

CoP and carbon was carried out using a mortar and pestle. The mass ratio of carbon and phosphide was 1:3.

## 2. Materials characterizations

The X-ray powder diffraction (XRD) patterns of the samples were obtained by the SmartLab X-ray diffractometer (Rigaku) with Cu K $\alpha$  radiation. Diffraction patterns were collected by step scanning in the 2 $\theta$  range of 10–80° with an interval of 0.02°. Field emission scanning electron microscopy (FE-SEM, Hitachi S-4800) was used to investigate the morphology of the materials. Elemental mapping was collected with the energy dispersive X-ray spectrometer (EDX) accessory of Hitachi SU8220 equipment. High resolution TEM (HRTEM) images were obtained by a JEM-F200 transmission electron microscope. The surface chemistry analysis was performed by X-ray photoelectron spectroscopy (XPS, ESCALab 250Xi Thermo Scientific) with Al K $\alpha$  (h $\nu$  = 1486.6 eV) radiation. And the base pressure of the analytical chamber was lower than 3.0 $\times$ 10<sup>-9</sup> mbar during the measurements. All binding energies were calibrated to an adventitious C1s peak at 284.8 eV. The deconvolution was carried out using the Thermo Avantage software package. A smart-type background subtraction and a Gaussian-Lorentzian peak shape were applied. Sample annealing was carried out in a tube furnace (Tanaka Experimental Furnace Co., LTD., SK-G05123 K).

## 3. Electrochemical measurement procedures

The catalysts studied here included Vulcan XC-72R, commercial Pt/C, NC, FeP-CoP + C and FeP-CoP + NC. The catalyst ink was prepared using the following recipe: 0.90 mL ethanol, 0.05 mL deionized water, 0.05 mL Nafion (5%wt) solution, 3mg catalyst powder. The ink was stirred by ultrasound for 6 hours at room temperature. The working electrode was a glassy carbon electrode (Gamry, USA) with  $\Phi$  = 5 mm ( $A$  = 0.196 cm<sup>2</sup>), the electrode was polished with 0.1  $\mu$ m, 0.3  $\mu$ m, 0.05  $\mu$ m particles of alumina powder, and washed well before use.

The electrochemical experiments were carried out in a classical three-electrode setup.

0.1 M KOH solution was used and stabilized at 25.0 °C in a water bath. CHI 760E electrochemical analyzer (CH Instrument Inc.) and the rotating disk electrode from Pine Instrument were used. The Hg/HgO electrode and Pt wire were used as the reference electrode and the counter electrode, respectively.

In ORR measurement, oxygen (99.999%) was first purged into the solution for 30 minutes to saturate the oxygen. The rotation speed of the RDE was 400, 625, 900, 1025, 1600, 2025 and 2500 rpm, the scanning rate was 10 mV s<sup>-1</sup> to obtain linear scanning voltammograms (LSV). The number of electrons transferred in the reaction was estimated by the Koutecký-Levich equation:

$$\frac{1}{J} = \frac{1}{B\omega^{-1/2}} + \frac{1}{J_k}$$

Where  $J$  is the measured disk current density (mA cm<sup>-2</sup>),  $J_k$  is the kinetic current density;  $\omega$  is the RDE rotation rate (rpm). The  $B$  is given by

$$B = 0.2nFC_0D_0^{2/3}V^{-1/6}$$

Where 0.2 is the arithmetic correction factor for in rpm,  $n$  is the number of electrons transferred per mol,  $F$  is Faraday constant (96,485 C cm<sup>-1</sup>),  $C_0$  is the concentration of dissolved O<sub>2</sub> (1.2 mM at 25 °C in 0.1 M KOH),  $D_0$  is the diffusion coefficient of O<sub>2</sub> (1.9×10<sup>-5</sup>cm<sup>2</sup> s<sup>-1</sup> at 25 °C in 0.1 M KOH), and  $V$  is the kinematic viscosity of the 0.1 M KOH electrolyte at 25 °C (0.01 m<sup>2</sup> s<sup>-1</sup>).

The Tafel slope was calculated using the Tafel equation:

$$\eta = b \log(j) + a$$

$\eta$ ,  $b$  and  $j$  represent the overpotential, Tafel slope and current density, respectively.

No iR compensation was applied. Chronoamperometry (CA) was used to test the corrosion resistance of the catalyst at a constant potential 2.0 V vs. RHE. The degradation of ORR and OER properties of the catalysts were tested after oxidation at a constant potential for 0.5 h. It should be noted that  $E_{\text{Hg/HgO}}$  is converted to the reversible hydrogen electrode (RHE) by the following formula:

$$E_{\text{RHE}} = E_{\text{Hg/HgO}} + 0.098 \text{ V} + 0.059 \times \text{pH}$$

#### 4. Differential electrochemical mass spectrometry (DEMS)

Mass signals were recorded using PFEIFFER QAS100 differential electrochemical mass spectrometry with a turbo pump (HIPACE 80, PFEIFFER). The key parameters of electron impact ionization, electron energy and emission current, were set as 70 eV and 2000  $\mu\text{A}$ , respectively. The gold-plated porous PTFE film (commonly known as gold film, its thickness of 25  $\mu\text{m}$ , porosity of 50%, pore size of 25 nm), which has permeability to volatile substances, was used to separate the electrolyte from the vacuum. Any volatiles generated from the electrode-electrolyte interface can be pumped into the mass spectrometer for analysis. The catalyst ink was coated on the gold film as the working electrode. A total of 80  $\mu\text{L}$  of catalyst ink was applied to the gold film via eight times of drop-casting. The working electrode area was 0.5  $\text{cm}^2$ . The counter electrode and reference electrode used were the same as those used in electrochemical measurements. Electrochemical impedance spectroscopy (EIS) was performed before the DEMS experiment. All spectra were recorded at 1.68 V vs. RHE with frequencies ranging from  $10^5$  Hz to 0.1 Hz at a voltage perturbation of 5 mV. The volatile products were detected while performing cyclic voltammetry (CV), multi-step potential (MSP) measurements. The voltage window of CV was 0.90–2.40 V vs. RHE with a scan speed of 10  $\text{mV s}^{-1}$ . The MSP was performed stepwise from 1.0 V to 2.40 V vs. RHE in eight stages, each lasting 10 minutes.

## 5. Supporting Figures

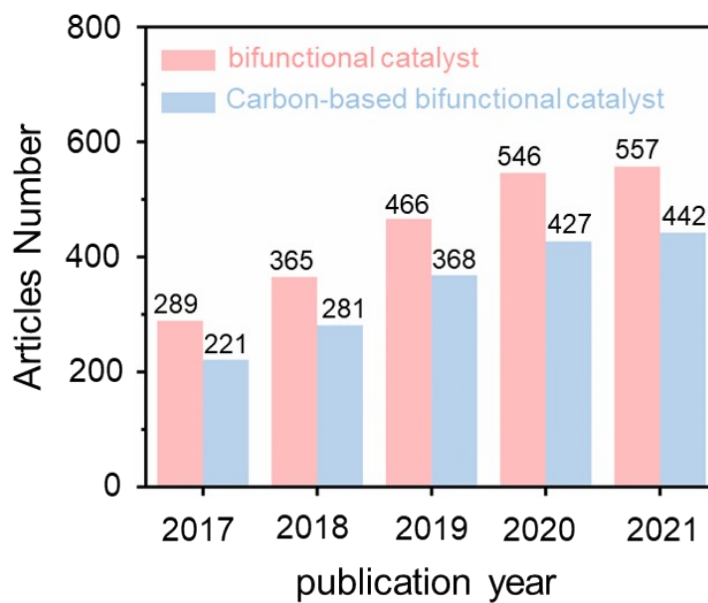


**Figure S1.** The research statistics about bifunctional and carbon-based bifunctional catalysts in recent years.

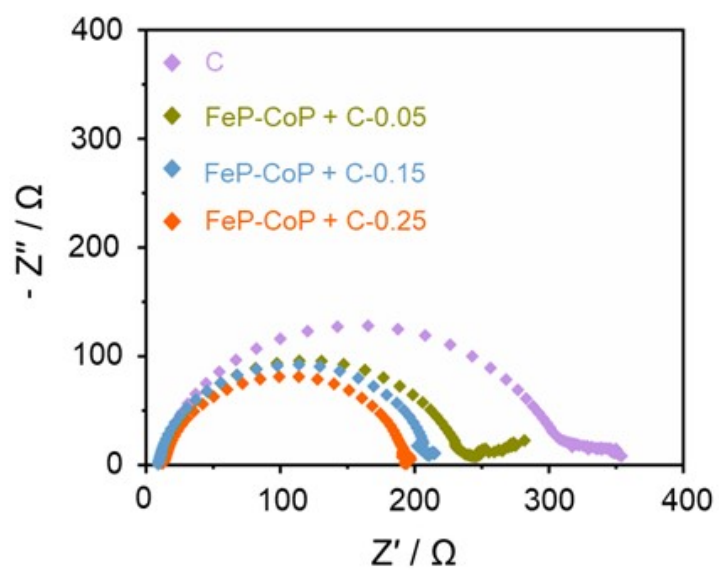


**Figure S2.** The Nyquist plot from the EIS measurement of carbons incorporated with different mass ratios to XC-72R (e.g., C-0.05 indicates the ratio of carbon is 5%).

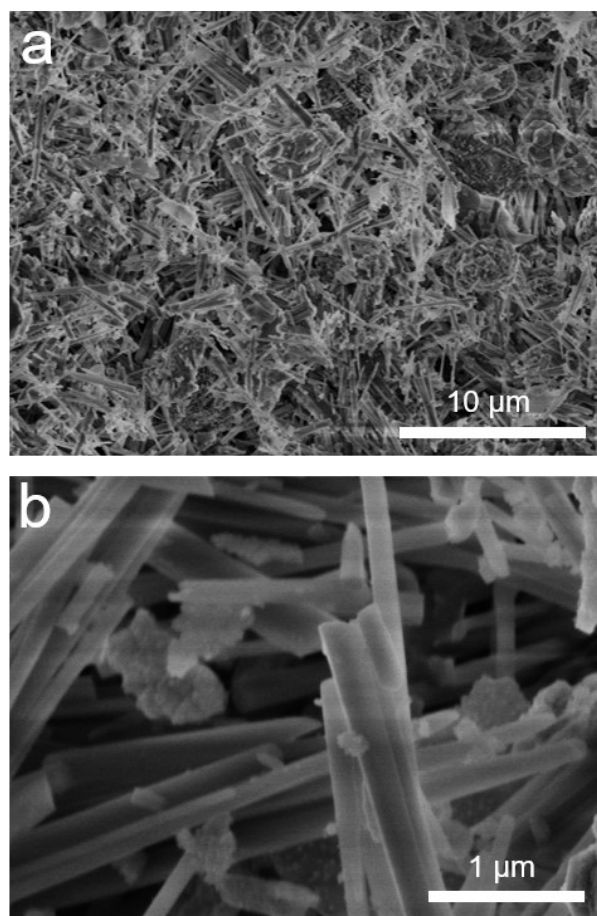


**Figure S3.** SEM images of  $\text{Fe}(\text{OH})_3\text{-Co}(\text{OH})_2$  precursor.



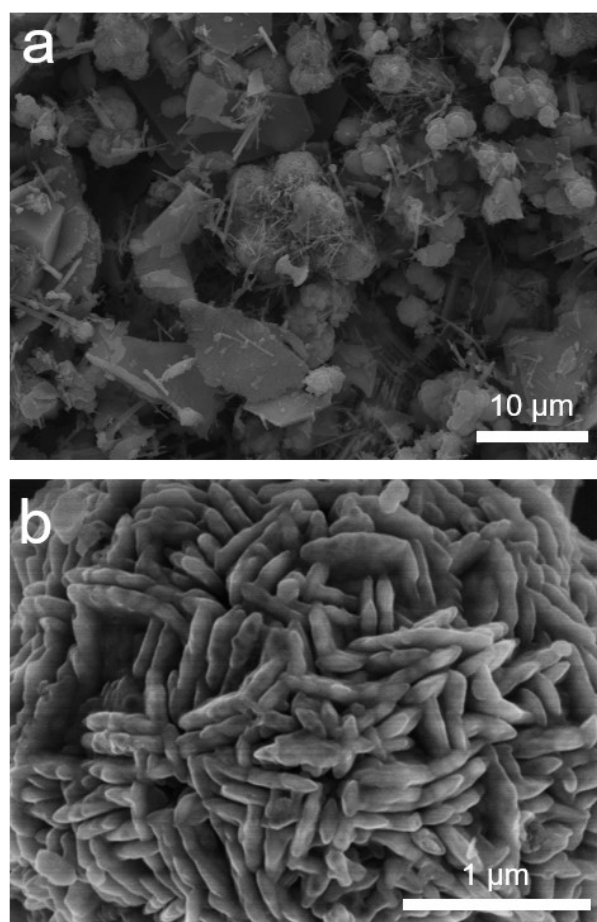


**Figure S4.** SEM images of FeP-CoP.

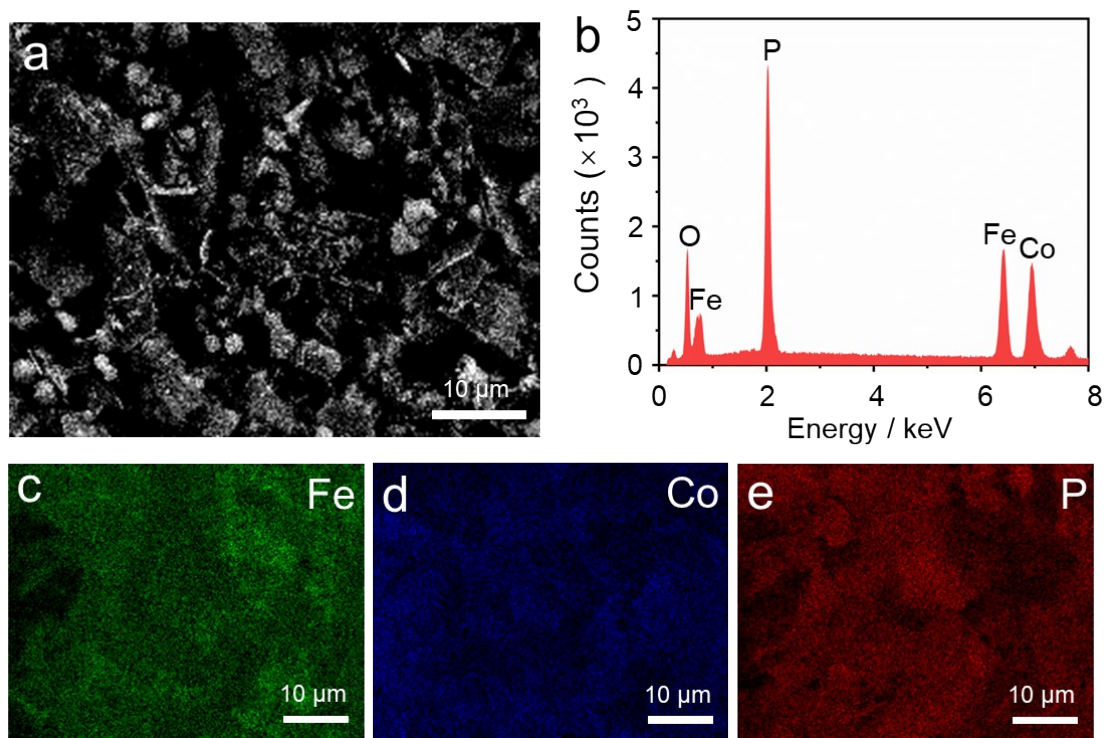


**Figure S5.** (a) SEM images of FeP-CoP, and the (b) corresponding EDX spectroscopy; (c-e) EDX elemental mappings of Fe, Co, and P.

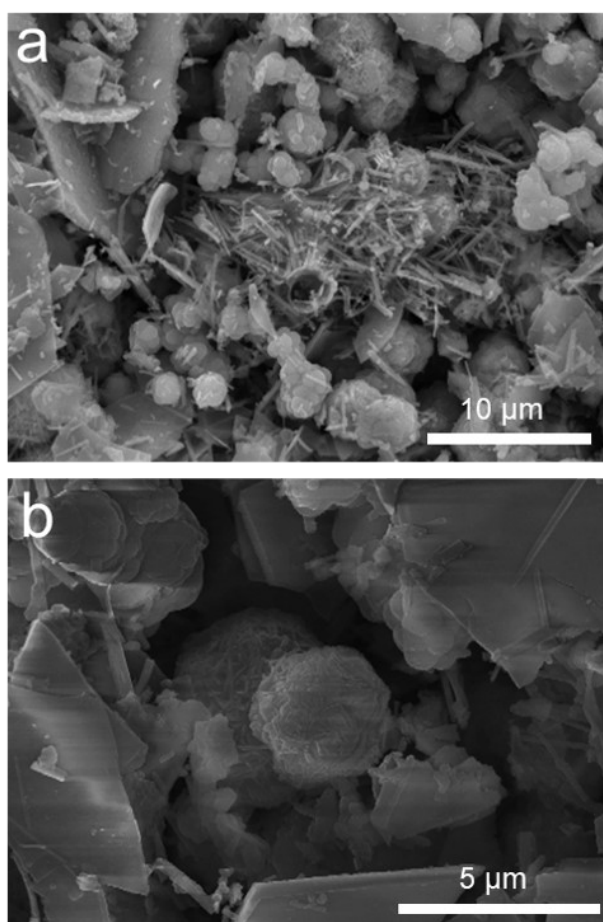


**Figure S6.** SEM images of FeP-CoP + C.

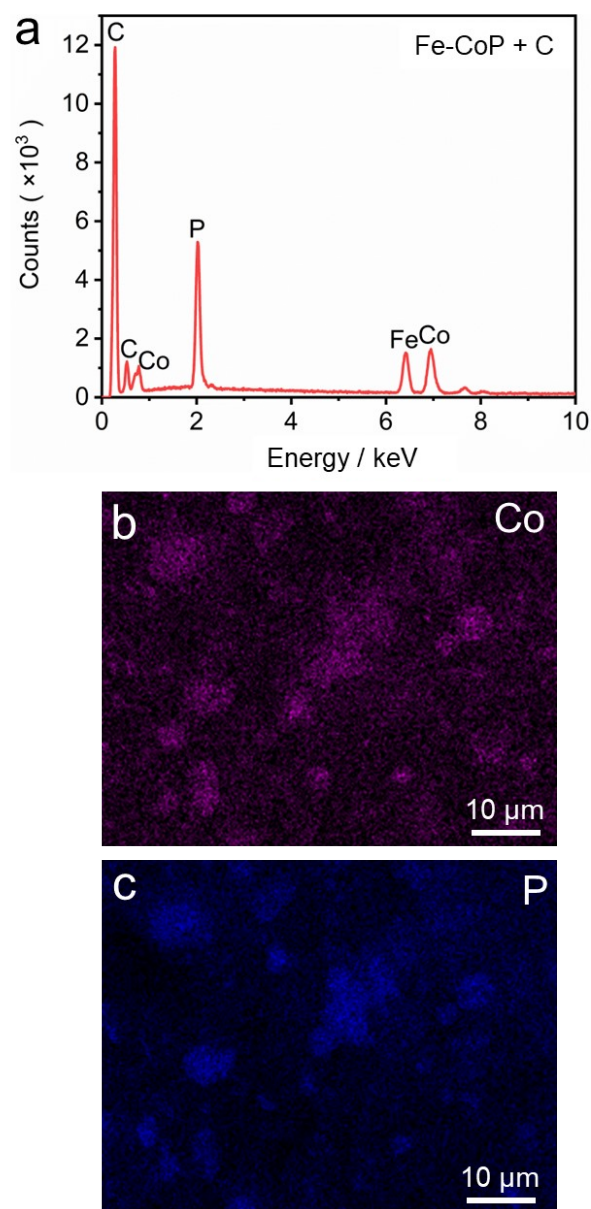


**Figure S7.** (a) EDX spectrum of FeP-CoP + C; (b-c) EDX elemental mappings of Co and P.

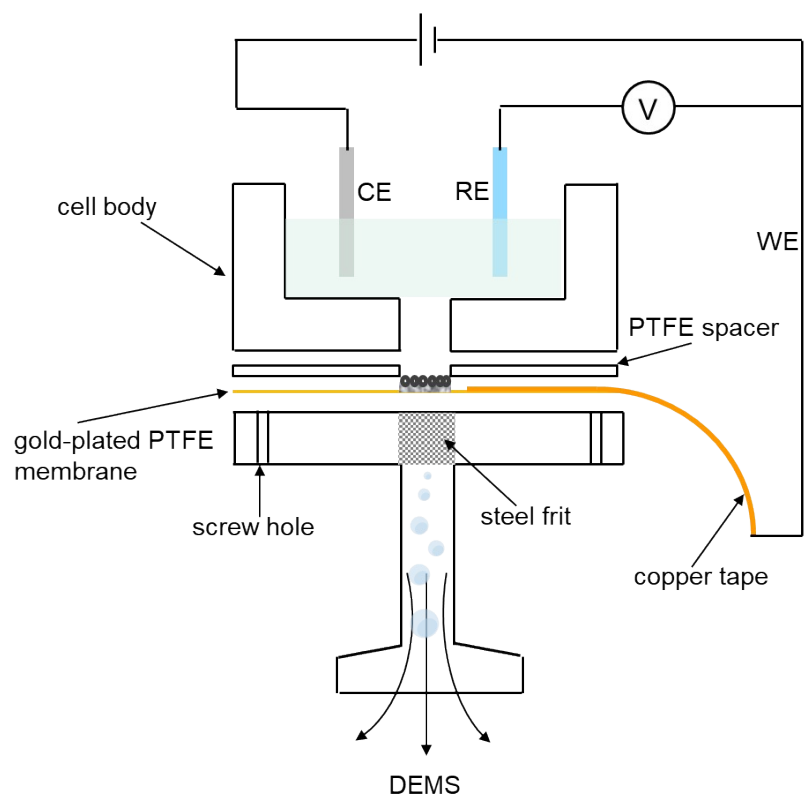


**Figure S8.** Schematic diagram of the online gold film DEMS configuration.

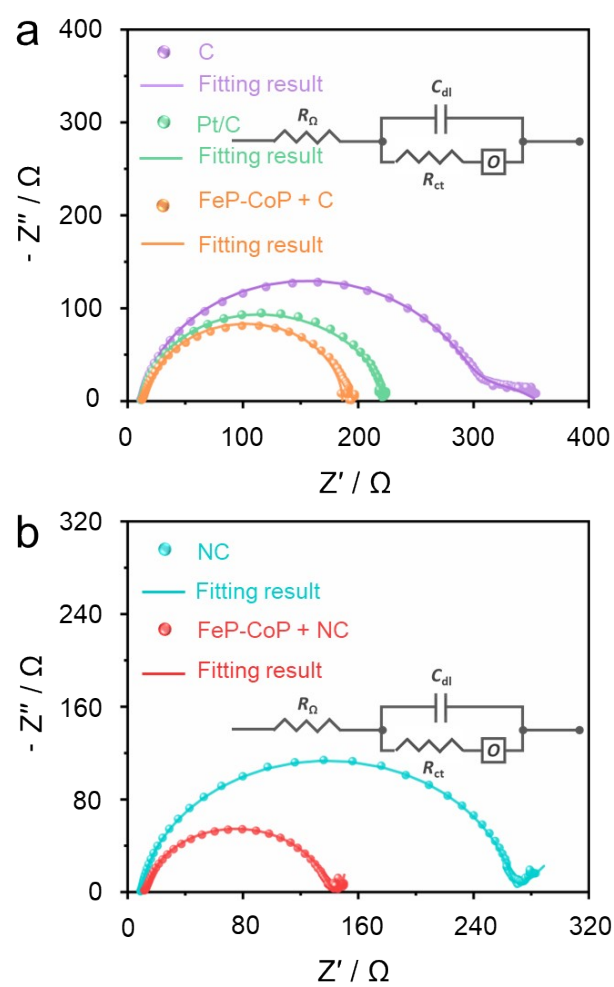


**Figure S9.** The fitted Nyquist plots from EIS measurement with the equivalent circuit.

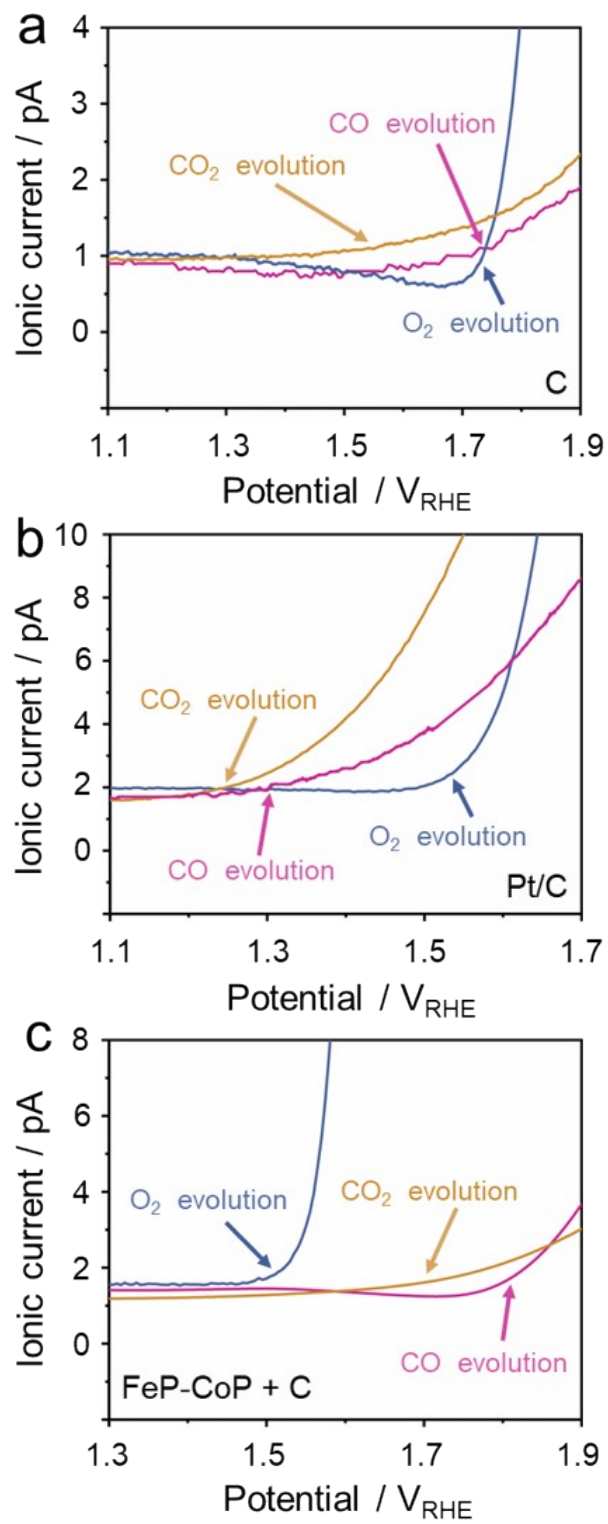


**Figure S10.** Details of  $O_2$ , CO and  $CO_2$  evolution potential for C, Pt/C and FeP-CoP + C.

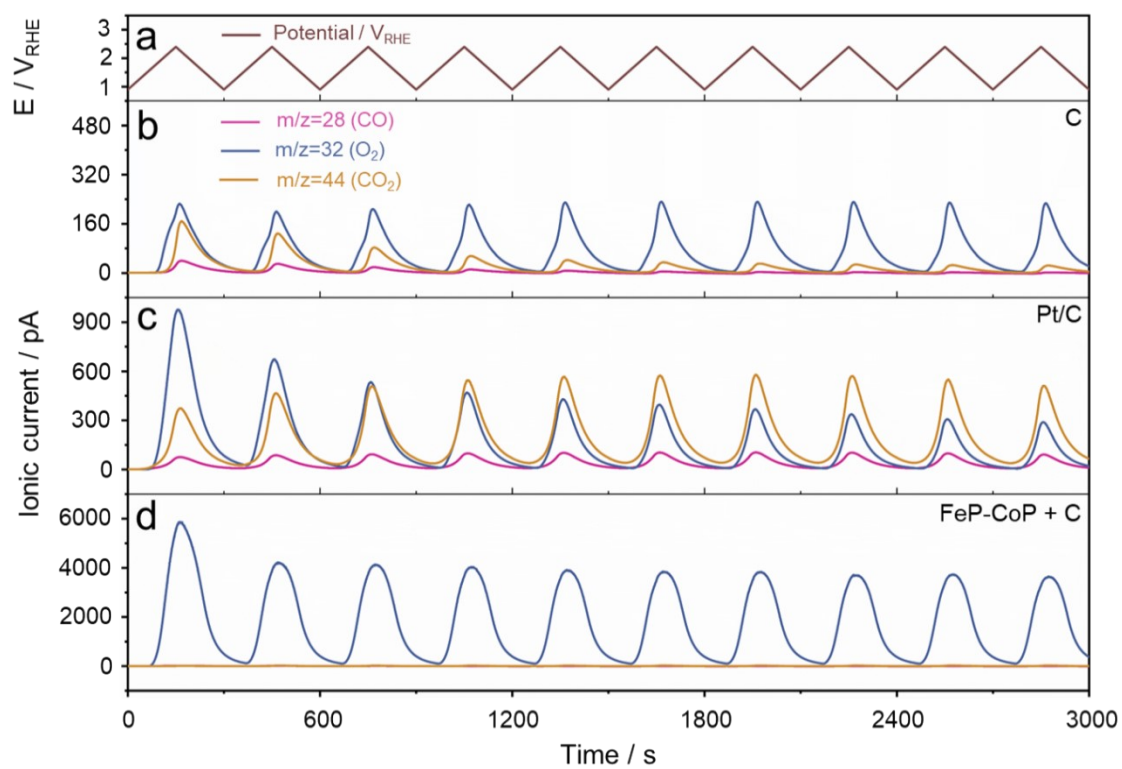


**Figure S11.** The ion current signals of different electrocatalysts in 0.1 M KOH electrolyte (10 cycles of CV): (a) potential protocol; (b-d) the ion current signals of CO ( $m/z = 28$ ),  $O_2$  ( $m/z = 32$ ) and  $CO_2$  ( $m/z = 44$ ) generated by different electrodes.



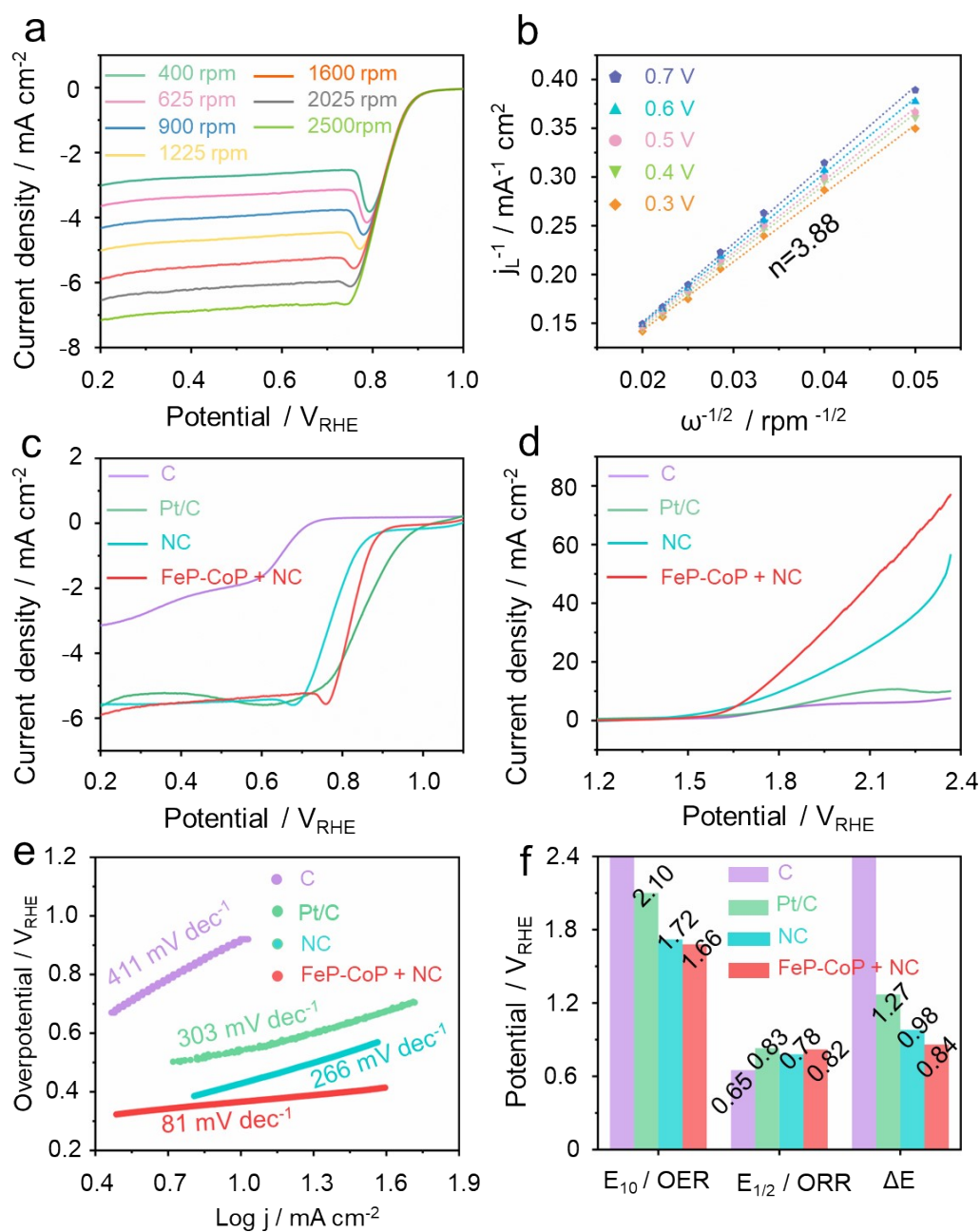


**Figure S12.** (a) LSV curves of FeP-CoP + NC at different rotation speeds; (b) Koutecky–Levich plot based on RDE data; (c-d) LSV curves of C, Pt/C, NC and FeP-CoP + NC at 1600 rpm for ORR and OER; (e) Tafel slopes of OER; (f) comparison of catalyst bifunctional performance. All experiments were carried at scanning rate of 10 mV s<sup>-1</sup> in a O<sub>2</sub>-saturated 0.1 M KOH electrolyte.

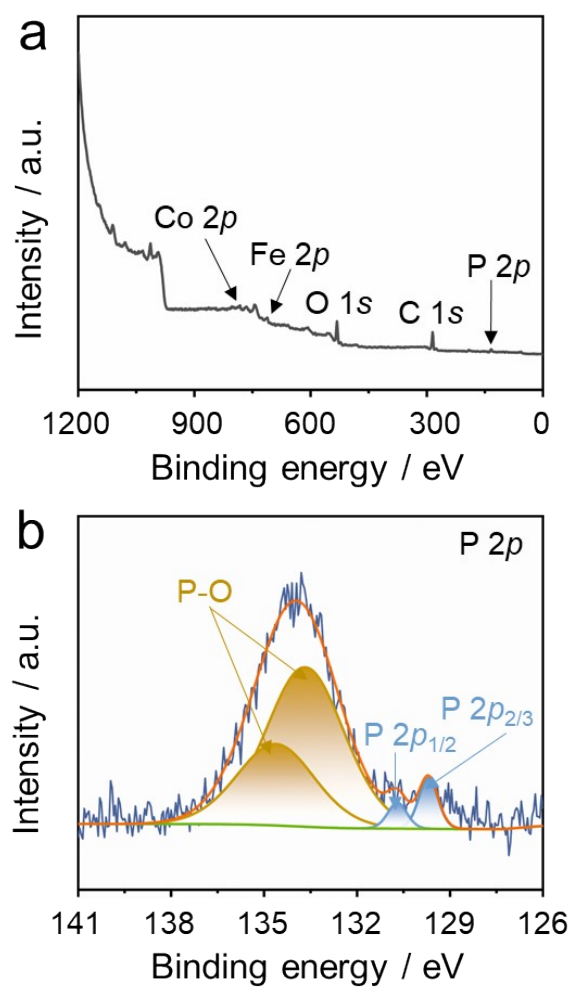


**Figure S13.** (a) XPS survey spectrum and high resolution XPS spectra of (b) P 2p, for FeP-CoP + C after 0.5 h @ 2.0 V<sub>RHE</sub> oxidation.

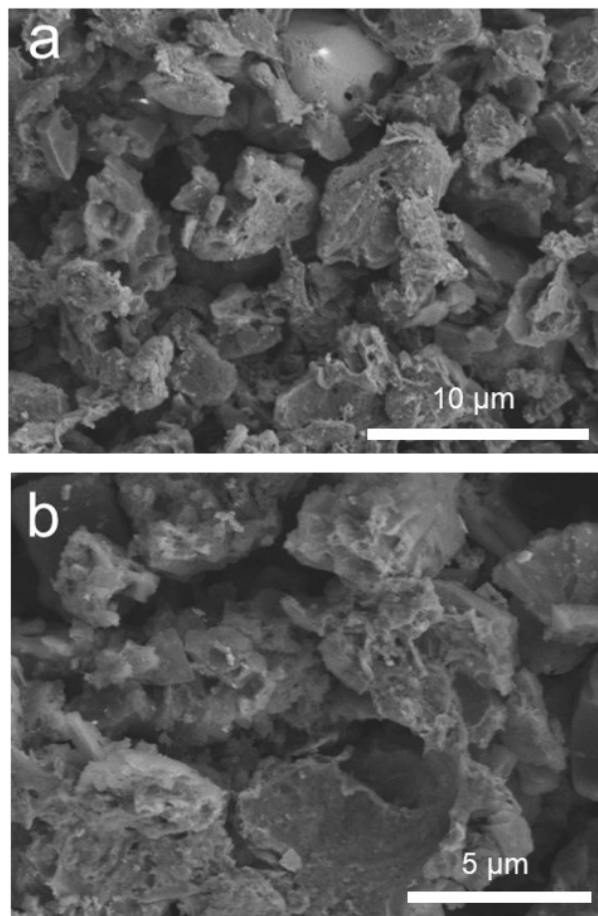


**Figure S14.** SEM images of FeP-CoP + NC after 0.5 h @ 2.0 V<sub>RHE</sub> oxidation.

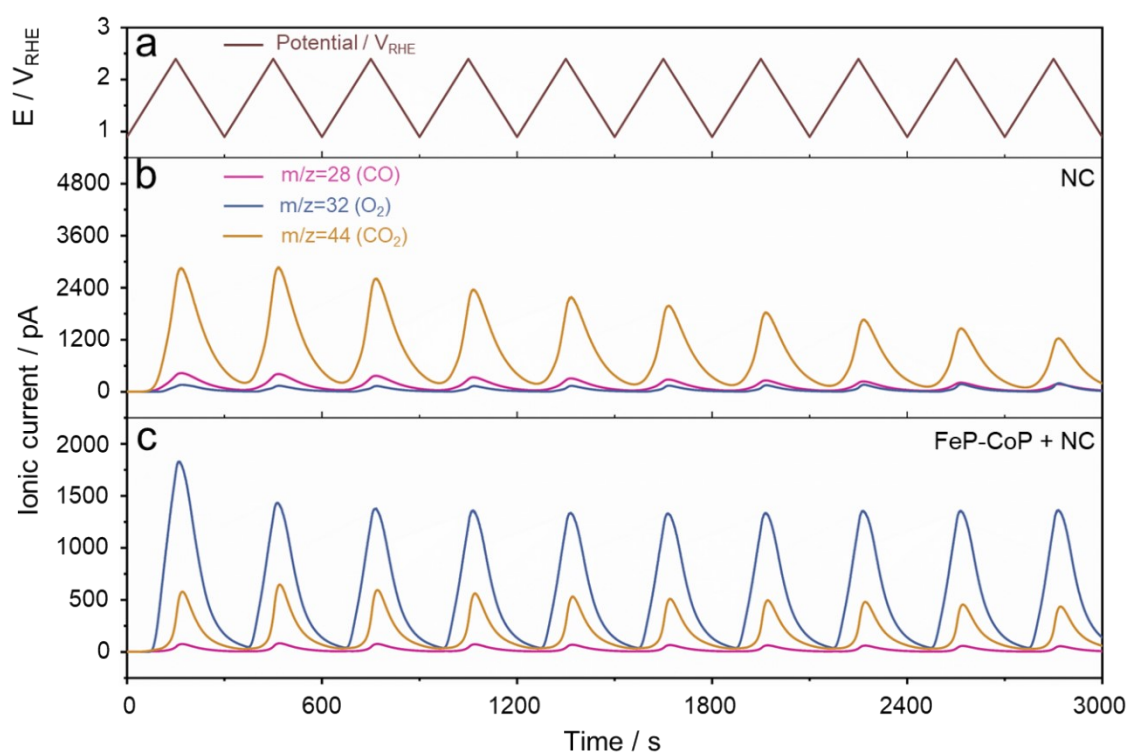


**Figure S15.** The ionic current signals of different electrocatalysts in 0.1 M KOH electrolyte (10 cycles of CV): (a) potential protocol; (b-d) the ion current signals of CO ( $m/z = 28$ ),  $O_2$  ( $m/z = 32$ ) and  $CO_2$  ( $m/z = 44$ ) generated by different electrodes.

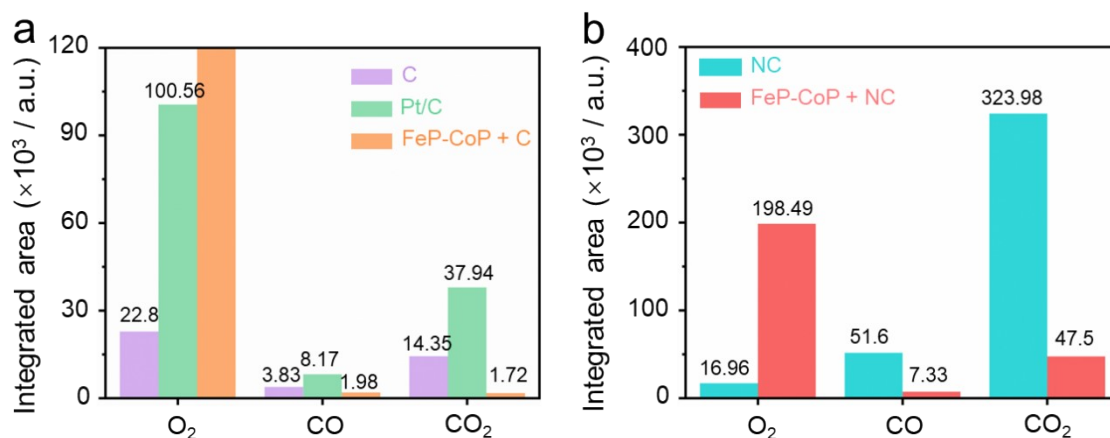


**Figure S16.** Integrated area of DEMS signals

## References

1. D. Eisenberg, W. Stroek, N. J. Geels, C. S. Sandu, A. Heller, N. Yan and G. Rothenberg, *Chem. Eur. J.*, 2016, **22**, 501-505.
2. X. Yan, Y. Zhao, J. Biemolt, K. Zhao, P. C. M. Laan, X. Cao and N. Yan, *J. Mater. Chem. A*, 2020, **8**, 7626-7632.
3. H. Baltruschat, *J. Am. Soc. Mass Spectrom.*, 2004, **15**, 1693-1706.
4. J. P. I. de Souza, S. L. Queiroz and F. C. Nart, *Quim. Nova*, 2000, **23**, 384-391.
5. W. Li and A. M. Lane, *Electrochem. Commun.*, 2009, **11**, 1187-1190.
6. O. Wolter and J. Heitbaum, *Ber. Bunsenges. Phys. Chem.*, 1984, **88**, 2-6.
7. S. Moeller, S. Barwe, J. Masa, D. Wintrich, S. Seisel, H. Baltruschat and W. Schuhmann, *Angew. Chem., Int. Ed.*, 2020, **59**, 1585-1589.
8. S. G. Ji, H. Kim, W. H. Lee, H.-S. Oh and C. H. Choi, *J. Mater. Chem. A*, 2021, **9**, 19834-19839.